International Immunopharmacology 76 (2019) 105835

Contents lists available at ScienceDirect

International Immunopharmacology

journal homepage: www.elsevier.com/locate/intimp

MicroRNA-124 alleviates the lung injury in mice with septic shock through inhibiting the activation of the MAPK signaling pathway by downregulating MAPK14

Weiyun Pan[a,1], Na Wei[b,1], Weiling Xu[c], Gang Wang[d], Fangchao Gong[e,*], Na Li[f,**]

[a] Department of ICU, The First Hospital of Jilin University, Changchun 130021, PR China
[b] Department of the First Operating Room, The First Hospital of Jilin University, Changchun 130021, PR China
[c] Department of Radiology, The First Hospital of Jilin University, Changchun 130021, PR China
[d] Department of the Second Operating Room, The First Hospital of Jilin University, Changchun 130021, PR China
[e] Department of Thoracic Surgery, The First Hospital of Jilin University, Changchun 130021, PR China
[f] Department of Neonatology, The First Hospital of Jilin University, Changchun 130021, PR China

ARTICLE INFO

Keywords:
MicroRNA-124
MAPK14
MAPK signaling pathway
Septic shock
Inflammatory response
Acute lung injury

ABSTRACT

Objective: Acute lung injury (ALI) is a severe lung disease with high mortality rate. Research has highlighted that the immune response to ALI is associated with significant changes in the expression of several microRNAs (miRNAs) in the lungs. In our research, we speculated that miR-124 moderated the severity of ALI through comprehensive suppression of the mitogen-activated protein kinase (MAPK) signaling pathway activation by targeting MAPK14.

Methods: A mouse model of ALI was established by array of experiments. The expression of MAPK14 and miR-124 was assessed in the tissues of ALI mice and the expression of inflammatory cytokines in ALI mice was determined. The expression of the related kinases in the MAPK signaling pathway and key cytokines in the pro-inflammatory response were assessed by a series of experiments. Immunohistochemistry and TUNEL staining were adopted to detect lung tissue cell proliferation and apoptosis in mice with ALI.

Results: MiR-124 was poorly expressed and MAPK14 was highly expressed in tissues of ALI mice. Overexpression of miR-124 or silence of MAPK14 alleviated the symptoms of ALI by down-regulating inflammatory cytokines expression, which could intrinsically suppress the expression of associated proteins in the MAPK signaling pathway and the downstream pro-inflammatory response factors, promote proliferation and inhibit apoptosis of lung tissue cells. Overexpression of MAPK14 inverted the phenotypic changes induced by overexpressing miR-124.

Conclusion: These results indicated that miR-124 could alleviate the symptoms of ALI by inhibiting the activation of MAPK signaling pathway via subsequent targeting of MAPK14. Additionally, miR-124 may serve as a useful biomarker to alleviate the severity of septic shock-induced lung injury.

1. Introduction

Septic shock is the most severe kind of sepsis, which is caused by infection [1]. It is a highly complex circulatory disease, which can be fatal, largely due to profound abnormalities in cells and metabolism [2]. Reports have flagged the progression of septic shock to acute lung injury (ALI). The infective site of septic shock has been used as a diagnostic modality to predict the outcome of patients with ALI [3]. Besides, ALI can lead to fulminant respiratory failure as well as death, which prevails with eminently high incidence and mortality rates [4]. The clinical and radiographic criteria are usually the bases of ALI diagnosis. However, due to a limitation of non-specificity of the criteria, the diagnosis is often uncertain [5]. Therefore, it is necessary to find new targets for the treatment of ALI.

A former study has highlighted the significance of inhibition of the activation of extracellular signal regulated kinase (ERK1/2) and p38

* Correspondence to: F. Gong, Department of Thoracic Surgery, The First Hospital of Jilin University, No. 71, Xinmin Street, Changchun 130021, Jilin Province, PR China.
** Correspondence to: N. Li, Department of Neonatology, The First Hospital of Jilin University, No. 71, Xinmin Street, Changchun 130021, Jilin Province, PR China.
E-mail address: gongfangchao@jlu.edu.cn (F. Gong), 414110808@qq.com (N. Li).
[1] These authors are regarded as co-first authors.

https://doi.org/10.1016/j.intimp.2019.105835
Received 18 April 2019; Received in revised form 8 August 2019; Accepted 17 August 2019
Available online 30 August 2019

mitogen-activated protein kinase (MAPK) as the regulating factors for ALI [6]. Reports have also indicated that p38 MAPK activation can result in lung inflammation and the pathological damage of lung tissue can be alleviated upon inhibition of p38 MAPK activation [7,8]. MAPK14 is a member of the p38 subfamily, vital for regulation of several transcription factors activation [9]. In our study, the findings demonstrated that MAPK14 was up-regulated in septic shock and ALI. Therefore, we intended to explore the involvement of MAPK14 in ALI with the underlying mechanism.

MicroRNAs (miRNAs) are a type of noncoding RNA molecules, which are of trivial functionality in controlling the gene expression in many developmental processes [10]. Several miRNAs have been reported to be necessary in the process of initiating, maintaining and resolving of ALI, and regulation of miRNAs may be considered as a potential strategy for ALI treatment [11]. Previous researches have showed that miR-124 can regulate cell proliferation and migration via regulation of the ERK/MAPK signaling pathway independent of SMAD [12]. Besides, miR-124 has been found to decrease greatly in lung adenocarcinoma and the proliferation, invasions and migration of human lung adenocarcinoma cells can be inhibited upon up-regulation of miR-124 [13]. So we speculated that miR-124 might inhibit the activation of MAPK signaling pathway by binding to MAPK14 to further alleviate ALI in mice with septic shock.

2. Materials and methods

2.1. Ethics statement

The study protocol was approved by the Experimental Animal Ethics Committee of The First Hospital of Jilin University. The animal experiments were strictly accordance with the principles to minimize the pain, suffering and discomfort to experimental animals.

2.2. Microarray-based analysis

The microarray datasets relevant to septic shock were retrieved from the Gene Expression Omnibus (https://www.ncbi.nlm.nih.gov/geo/). Three datasets GSE2644, GSE13904 and GSE26378 (Table 1) were used to screen for the differentially expressed genes (DEGs). The affy package (http://www.bioconductor.org/packages/release/bioc/html/affy.html) in the R Language Programming was employed for conducting background correction and standardized pretreatment of the gene expression data. Limma package (http://master.bioconductor.org/packages/release/bioc/html/limma.html) was adopted to screen the DEGs between the normal individuals and patients with septic shock with $|\log2 \text{ Fold Change}| > 2.0$ and *adj.P.Val* (*p* value after correction) < 0.05 as the threshold. Additionally, the expression heatmap of DEGs was drawn using the pheatmap package (https://cran.r-project.org/web/packages/pheatmap/index.html). The jvenn (http://jvenn.toulouse.inra.fr/app/example.html) was employed to compare the DEGs from three microarray datasets respectively. On the basis of the protein-protein interaction (PPI) information specified by the String database (https://string-db.org/) [14], PPI network of the DEGs was retrieved by mean of the Cytoscape 3.6.0 software [15]. miRTarBase (http://mirtarbase.mbc.nctu.edu.tw/php/search.php), miRSearch (http://www.exiqon.com/microrna-target-prediction), miRDB (http://www.mirdb.org/), RNA22 (https://cm.jefferson.edu/rna22/), DIANA (http://diana.imis.athena-innovation.gr/DianaTools/index.php?r=microT_CDS/index), and miRWalk (http://mirwalk.umm.uni-heidelberg.de/) were used to predict the potential regulatory miRNA of the respective DEGs, after which the prediction results were compared.

2.3. Dual-luciferase reporter gene assay

In order to verify whether MAPK14 is a direct target gene of miR-124, the synthesized 3′-untranslated region (3′UTR) of MAPK14 was inserted into the pMIR-reporter (Beijing Huayueyang Biotechnology Co., Ltd., Beijing, China) (MAPK14-WT). The mutant form in which the potential miR-124 binding sites were mutated was also inserted into the pMIR-reporter (MAPK14-MUT). The luciferase reporter plasmids (MAPK14-WT and MAPK14-MUT) were separately co-transfected with miR-124 and renilla luciferase plasmid into HEK293T cells, respectively. After 48 h, the cells were collected and lysed. The luciferase activity of cells was measured using a luciferase assay kit (K801-200, BioVision, San Francisco, CA, USA) on the Glomax20/20 luminometer (Promega Corp., Madison, Wisconsin, USA).

2.4. Establishment of a mouse model of lipopolysaccharides (LPS)-induced ALI

Sixty-five healthy specific pathogen-free Institute of Cancer Research (ICR) mice (aged 6-weeks old and weighing 20–23 g) were acquired from Hunan SJA Laboratory Animal Co., Ltd. (Changsha, Hunan, China). A total of 55 randomly-selected ICR mice were injected with standard strain suspension (5 mg/kg) of *Escherichia coli* LPS (Sigma Aldrich, St. Louis, MO, USA) via the tail vein under sterile conditions to induce the mouse model of ALI and the remaining 10 normal mice did not receive any treatment.

Among 55 mice chosen for LPS-induced ALI model establishment, 12 mice did not undergo any treatment, whereas the remaining mice were respectively injected with NC plasmid (n = 13), miR-124 mimic (n = 10), si-MAPK14 (n = 10), or both miR-124 mimic and oe-MAPK14 (n = 10) via the tail vein. The sequence of si-MAPK14 was 5′-GCTTC AGCAGATAATGCGT-3′. The aforementioned plasmids (20 μg for each) were purchased from Dharmacon Corporation (Lafayette, CO, USA). The plasmids were diluted to a concentration of 5 μg/μL using RNA-free H_2O, and then mixed with 3.2 μL in vivo-jet PEITM (PT-201-10G, Polyplus-transfection, Strasbourg, France) and 5% glucose solution to attain a final volume of 50 μL. After 15 min of incubation at room temperature, the prepared solution was injected into the mice via the tail vein [16,17]. Normal mice were injected with an equivalent amount of 5% glucose solution. During the operation, 2 mice receiving no treatments and 3 mice injected with blank plasmid died.

2.5. Lung wet/dry (W/D) weight ratio detection

Three mice were randomly chosen from each group, anaesthetized by 4% sodium pentobarbital (400 mg/kg) and finally euthanized by cervical dislocation. The lungs were extracted and weighed (wet weight). The lung tissues were then dried at 80 °C for 48 h and weighed (dry weight). The W/D weight ratio was calculated according to the formula: W/D = wet weight / dry weight.

Table 1
Microarray datasets of septic shock genes.

Accession	Platform	Organism	Tissue	Sample
GSE2644	GPL570	Homo sapiens	Whole blood	98 children with septic shock and 32 normal controls
GSE13904	GPL570	Homo sapiens	Whole blood	18 normal children and 106 children with septic shock
GSE26378	GPL570	Homo sapiens	Whole blood	82 children with septic shock and 21 normal controls

2.6. Hematoxylin-eosin (HE) staining

The lung tissues were fixed in a conventional manner using 10% neutral formaldehyde solution for 24 h, dehydrated with gradient alcohol, permeabilized using xylene, paraffin-embedded, and then sliced into 4-μm sections. Subsequently, the sections were dehydrated using gradient alcohol, permeabilized using xylene, and stained with hematoxylin (H8070-5g, Beijing Solarbio Science & Technology Co., Ltd., Beijing, China) for 4 min. After differentiation using hydrochloric acid alcohol for 10 s, the sections were stained using eosin (PT001, Shanghai Bogoo Biotechnology Co., Ltd., Shanghai, China) for 2 min, dehydrated using gradient alcohol, permeabilized using xylene, and finally mounted using neutral balsam. The histopathological changes of lung tissues were observed under an optical microscope (DMM-300D, Shanghai Caikon Optical Instrument Co., Ltd., Shanghai, China).

2.7. Immunohistochemistry (IHC)

The lung tissue specimens were fixed using formaldehyde, paraffin-embedded, and cut into 4-μm serial sections. After high-pressure antigen retrieval, the sections were blocked with 10% normal goat serum (Beijing ComWin Biotech Co., Ltd., Beijing, China), and incubated overnight at 4 °C with the rabbit anti-mouse monoclonal antibody to MAPK14 (1:500, bs-28027R, Beijing Bioss Antibodies Co., Ltd., Beijing, China) and Ki67 TH (ab15580, 1:5000, Abcam Inc., Shanghai, China), followed by another 30 min regimen of incubation at 37 °C with addition of the biotin-labeled goat anti-rabbit immunoglobulin G (IgG, 1:1000, a6721, Abcam Inc., Cambridge, MA, USA). After the addition of streptomycin avidin-peroxidase solution (Beijing Zhongshan Biotechnology Co., Ltd., Beijing, China), the sections were developed using diaminobenzidine (DA1010-3mL, Beijing Solarbio Science & Technology Co., Ltd., Beijing, China) for 5–10 min. The sections were then immersed in hematoxylin, rinsed with 1% hydrochloric acid alcohol, treated using 1% ammonia, followed by dehydration using gradient alcohol, permeabilization using xylene, and subsequently sealed with neutral balsam. Five high-power visual fields were randomly chosen from each section to determinate the positive staining area, positive staining area percentage and the average integrated optical density or average intensity.

2.8. Reverse transcription quantitative polymerase chain reaction (RT-qPCR)

Total RNA was extracted in strict accordance to the provided instructions of the Trizol kit (Invitrogen, Carlsbad, CA, USA). RNA was then reversely transcribed into cDNA using the PrimeScript RT Kit (RR014A, Takara Biomedical Technology Co., Ltd., Beijing, China). Fluorescent qPCR was performed in strict accordance with the protocols of the SYBR® Premix Ex Taq™ II kit (RR820A, Action-award Co., Ltd., Guangzhou, Guangdong, China) using the ABI PRISM® 7300 system (Applied Biosystems Inc., Carlsbad, CA, USA). U6 was regarded as an internal reference for miR-124 while β-actin served for the other genes. All primers (Table 2) were synthesized by the Wuhan Bojie Biological Engineering Co., Ltd., (Wuhan, Hubei, China). The relative expression of gene was calculated on the basis of the $2^{-\Delta\Delta Ct}$ method.

2.9. Western blot analysis

Mouse tissues were lysed conventionally using the Radio Immunoprecipitation Assay lysis buffer containing phenylmethylsulfonyl fluoride on ice and centrifuged to collect the supernatant. The total protein concentration was assessed following the provided instructions of the bicinchoninic acid protein assay kit. Proteins were subjected to sodium dodecyl sulfate-polyacrylamide gel electrophoresis and then transferred onto polyvinylidene fluoride membranes. The membranes were blocked with 5% skimmed milk for 1 h at room temperature and incubated overnight with the following diluted primary antibodies: mouse monoclonal antibody to MAPK14 (sc-271120, 1:500, Santa Cruz Biotechnology Inc., Santa Cruz, CA, USA), rabbit anti-mouse polyclonal antibody to p-MAPK14 (ab47363, 1:1000), rabbit anti-mouse polyclonal antibody to ERK (ab184699, 1:10,000), rabbit anti-mouse polyclonal antibody to p-ERK (ab201015, 1:1000) and cyclooxygenase-2 (COX-2, ab15191, 1:1000). Afterwards, the membranes were incubated with the horseradish peroxidase (HRP)-labeled goat anti-mouse IgG H&L (ab205719, 1:10,000) goat anti-rabbit IgG H&L (ab6721, 1:2000) for 1 h at 37 °C. The aforementioned antibodies were acquired from Abcam Inc. (Cambridge, MA, USA) except for MAPK14. The membrane was immersed in enhanced chemiluminescence solution (Pierce, Waltham, MA, USA) for 1 min at room temperature, covered with a preservative film and eventually developed in the dark. With β-actin (ab8227, 1:1000, Abcam Inc., Cambridge, MA, USA) as an internal control, the relative expression of the proteins was expressed as the ratio of gray value of the target band to that of the internal control band.

Table 2
Primer sequence for reverse transcription quantitative polymerase chain reaction.

Name	Primer sequence (5′–3′)
miR-124	F: GCCGATTCCATCGCGTTCCCCAAA- R: GCCGGATCCAGGGATGAAGGGTGCTGGCCT
MAPK14	F: ACCTTGCCACTTTGGCTTCT R: ATGCATGGCTGAGGGATAGC
U6	F: GCGCGTCGTGAAGCGTTC R: GTGCAGGGTCCGAGGT
β-Actin	F: TTGATGCTTGGTGGGTGGTTR R: CGATCCACACGGAGTACTTG
ERK	F: CCCCCAGTTCTTTACCCTGG R: TGCATTGAAAGTGCACACTGC
COX-2	F: GAACAACATTCCCTTCCTTGG R: GAAGTTCCTTATTCCTTTCACACC

Note: F, forward; R, reverse; miR-124, microRNA-124; MAPK, mitogen-activated protein kinase; ERK, extracellular signal-regulated kinase; COX-2: cyclooxygenase 2.

2.10. Enzyme-linked immunosorbent assay (ELISA)

Then, 24 h after modeling, 0.5 mL blood was collected and transferred into the serum separator tube. The blood was coagulated for 10–20 min at room temperature, and then subjected to centrifugation at 1000 ×*g* for 20 min and the supernatant collected. The expression levels of several inflammatory cytokines interleukin-(IL-)6, IL-10, tumor necrosis factor-α (TNF-α), IL-1β in mice serum were detected in strict accordance with the provided instructions of ELISA kits: IL-6 (ab100712), IL-10 (ab46103), TNF-α (ab100747), and IL-1β (ab197742) (Abcam, Cambridge, MA, USA). Optical density value of each sample was measured within 3 min using a microplate reader (BioTek Instruments Inc., Winooski, VT, USA) at a wavelength of 450 nm.

2.11. Terminal deoxynucleotidyl transferase (TdT)-mediated 2′-deoxyuridine 5′-triphosphate (dUTP)-digoxigenin nick end labelling (TUNEL) staining

The tissue sections were deparaffinized and permeabilized for 30 min using Protease K. The sections were then blocked with bovine serum albumin (1 mg/mL) in 50 mM Tris-HCl for 10 min at 37 °C. The TUNEL positive cells were detected using the in situ cell death detection kit (Roche, Indianapolis, IN, USA). The nucleus was counterstained using 6-diamidino-2-phenylindole (Roche, Indianapolis, IN). The sections were then observed under the Zeiss microscope (Carl Zeiss AG, Jena, Germany) under randomly selected 10 visual fields, from which

the apoptosis rate was calculated.

2.12. Statistical analysis

Statistical analysis was conducted using the SPSS 21.0 statistical software (IBM Corp. Armonk, NY, USA). Measurement data were expressed as mean ± standard deviation. The unpaired *t*-test was adopted to compare data between two groups of unpaired design that conformed to normal distribution and homogeneity of variance. Comparisons of data between multiple groups were conducted by one-way analysis of variance (ANOVA) and subjected to Tukey's post hoc test. The data at different time points were analyzed by repeated measures ANOVA, followed by Tukey's post hoc test. A value of $p < 0.05$ was considered to be of statistical significance.

3. Results

3.1. miR-124 and MAPK14 may participate in the development of septic shock

Microarray-based analysis was performed to screen for septic shock-related DEGs from the selected microarray datasets of septic shock (GSE2644, GSE13904 and GSE26378) using R language. The Venn map was constructed using an evaluative comparison of the top 150 DEGs from each microarray dataset (Fig. 1A), which led to the identification of 63 intersected genes. Based on provided PPI information from the String database, the PPI network of septic shock-related DEGs was established (Fig. 1B), ascertaining the strong association of MAPK14 gene with other genes, thereby speculating MAPK14 to be of trivial importance in septic shock. The expression heatmaps of the top 60 DEGs from GSE13904 and GSE26378 were drawn (Fig. 1C–D). It was revealed that the expression of MAPK14 in patients with septic shock was higher than the normal individuals. Besides, the expression profile of GSE2644 depicted that MAPK14 was aberrantly highly expressed in patients with septic shock (Fig. 1E), further indicating that MAPK4 might be involved in the development of septic shock. The miRTarBase, miRSearch, miRDB, RNA22, DIANA and miRWalk databases were used to predict the miRNA that could potentially target MAPK14. A comparison of the prediction results from the aforementioned databases suggested that only mmu-miR-124-3p was in the intersection (Fig. 1F), indicating that miR-124 was likely to regulate MAPK14.

3.2. MAPK14 is a target gene of miR-124

To confirm whether miR-124 could target MAPK14, the binding site between miR-124 and MAPK14 was predicted on the basis of the online bioinformatics website (http://www.targetscan.org/vert_71/). As shown in Fig. 2A, the potential binding sites of miR-124 were evident in the 3′UTR of MAPK14, herein suggesting that MAPK14 was conceivably a target gene of miR-124. Moreover, the results of dual-luciferase reporter gene assay (Fig. 2B) showed that compared with mimic control, miR-124 mimic notably attenuated the luciferase activity of MAPK14-WT ($p < 0.05$) with no influence on the luciferase activity of MAPK14-MUT ($p > 0.05$), indicating that miR-124 could specifically bind to MAPK14 mRNA and down-regulate the expression of MAPK14 gene. Conjointly, these findings demonstrated that miR-124 could target and negatively regulate MAPK14.

3.3. LPS-induced ALI mice present up-regulated MAPK14 and down-regulated miR-124 in lung tissues

Moreover, the expression of MAPK14 and miR-124 in liver, kidney, pancreas and lung tissues of LPS-induced ALI mice was measured by subsequent RT-qPCR. Fig. 3A–B manifested that MAPK14 expression visibly increased ($p < 0.05$) while the miR-124 expression visibly decreased in liver, kidney, pancreas and lung tissues from LPS-induced ALI mice ($p < 0.05$) in comparison to the tissues from normal mice, with significant alterations in lung tissues. Therefore the expression of MAPK14 was high while the expression of miR-124 was low in lung tissues from LPS-induced ALI mice, which was consistent with the bioinformatics analysis as well as the results of dual-luciferase reporter gene assay.

3.4. miR-124 downregulates MAPK14 expression to alleviate inflammatory response in LPS-induced ALI mice

To further explore the function of miR-124 and MAPK14 in ALI, LPS-induced ALI mice were treated with the blank plasmid, miR-124 mimic, si-MAPK14, or oe-MAPK14, and the expression of inflammatory cytokines (TNF-α, IL-6, IL-1β, and IL-10) in serum were detected using ELISA. Fig. 4 showed that the expression of inflammatory cytokines evidently decreased in ALI mice injected with miR-124 mimic or si-MAPK14 ($p < 0.05$), with potential blockade by co-injection of oe-MAPK14, indicating that overexpressing miR-124 or silencing MAPK14 could lower the expression of inflammatory cytokines, thus meticulously attenuating the inflammatory response in LPS-induced ALI mice.

3.5. Elevating miR-124 or depleting MAPK14 ameliorates lung injury in ALI mice induced with LPS

Then the regulatory effects of miR-124 and MAPK4 in LPS-induced ALI mice were determined. The W/D ratio of lung tissue was calculated to compare the degree of pulmonary edema (Fig. 5A), which demonstrated an attenuated degree of pulmonary edema in ALI mice treated with miR-124 mimic or si-MAPK14 ($p < 0.05$), which was reversed by co-treatment. Therefore, overexpressing miR-124 could ameliorate the degree of lung injury in ALI mice induced with LPS by downregulating MAPK14.

Additionally, HE staining was conducted to evaluate the pathological changes of lung tissues in ALI mice induced with LPS (Fig. 5B–C). Following the injection of LPS, ALI mice exhibited markedly widened alveolar septa, red blood cell exudation and inflammatory cell infiltration, which could be salvaged by miR-124 mimic or si-MAPK14. However, the co-expression of miR-124 mimic and oe-MAPK14 failed to rescue the pathological changes in ALI mice. The aforementioned results elucidated that overexpressing miR-124 could attenuate the degree of lung injury in ALI mice induced with LPS by reducing the expression of MAPK14.

Further, the assessment of the expression of MAPK14 protein in lung injury tissues of ALI mice induced with LPS was conducted by IHC (Fig. 5D). No significant difference was observed between the ALI mice treated with blank plasmid or both miR-124 mimic and oe-MAPK14 relative to the ALI mice without treatment ($p > 0.05$). However, the MAPK14 protein positive rate was down-regulated in response to miR-124 mimic treatment and si-MAPK14 treatment ($p < 0.05$). Therefore, these findings illustrated that overexpression of miR-124 and silence of MAPK14 in ALI mice induced with LPS could decrease the expression of MAPK14 protein. In summary, overexpression of miR-124 or silence MAPK14 alleviated the lung injury of ALI mice.

3.6. miR-124 alleviates lung injury in ALI mice induced with LPS by inactivating the MAPK signaling pathway

Since miR-124 could potentially alleviate lung injury in ALI mice by decreasing MAPK14, the aim shifted at exploring the impact on the MAPK signaling pathway. RT-qPCR was performed to assess the expression of key kinases (MAPK14 and ERK1/2) in the MAPK signaling pathway and the key enzyme (COX-2) of pro-inflammatory response (Fig. 6A). The results indicated that the expression of MAPK14, ERK1/2, and COX-2 had reduced evidently in response to miR-124 mimic in ALI mice ($p < 0.05$).

Moreover, Western blot analysis was conducted in order to examine

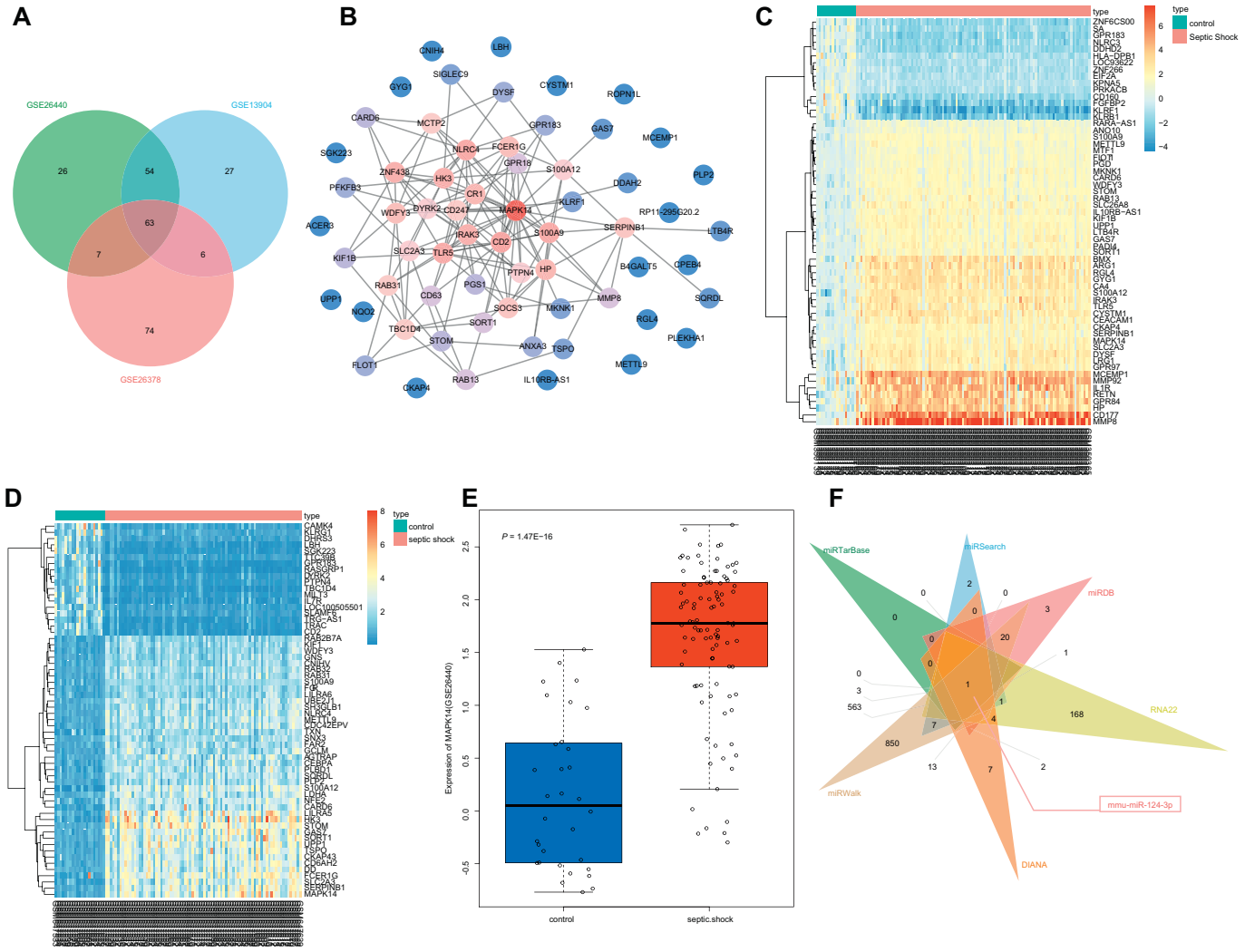

Fig. 1. Bioinformatics analysis identified miR-124 and MAPK14 in the progression of septic shock. A. top 150 differentially expressed genes retrieved from the septic shock-related microarray datasets of GSE2644, GSE13904 and GSE26378. B. PPI network of septic shock-related differentially expressed genes. C–D. expression heatmap of the top 60 differentially expressed genes from septic shock-related microarray datasets of GSE13904 and GSE26378, in which the abscissa was reflective of the sample numbers, the ordinate was reflective of the differential expressed genes, the histogram in the upper right is color gradation. Each rectangle corresponds to the expression of a sample. E. expression changes of MAPK14 in GSE2644. F. prediction results of the miRNA targeting MAPK14 by miRTarBase, miRSearch, miRDB, RNA22, DIANA and miRWalk databases.

protein levels of MAPK14, ERK1/2, COX-2, as well as the phosphorylation levels of ERK1/2. Fig. 6B–C demonstrated that the phosphorylation levels of ERK1/2 decreased evidently in response to miR-124 mimic in ALI mice ($p < 0.05$), indicating the inactivation of the MAPK pathway. So, it was concluded that up-regulation of miR-124 could inactivate the MAPK signaling pathway.

3.7. Overexpression of miR-124 or silence of MAPK14 promotes lung cell proliferation and inhibits lung cell apoptosis of mice in ALI mice induced with LPS

Here, the regulatory roles of miR-124 and MAPK14 in lung cell proliferation and apoptosis were investigated. Cell proliferation in lung

A

	Predicted consequential pairing of target region (top) and miRNA (bottom)	Site type	Context++ score
Position 545-552 of MAPK14 3' UTR	5' . . . ACUGUCAGUCUGUUUGUGCCUUA. . .	8mer	-0.54
hsa-miR-124-3p.1	3' CCGUAAGUGGCGCACGGAAU		

	Predicted consequential pairing of target region (top) and miRNA (bottom)	Site type	Context++ score
Position 604-611 of MAPK14 3' UTR	5' . . . ACUGUAAAUAUGUUUGUGCCUUA. . .	8mer	-0.50
hsa-miR-124-3p.1	3' CCGUAAGUGGCGCACGGAAU		

B

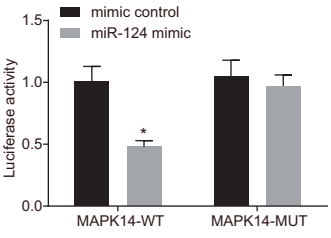

Fig. 2. miR-124 specifically binds to MAPK14 mRNA and down-regulates its expression. A. the binding site between miR-124 and MAPK14 predicted by an online bioinformatics website. B. luciferase activity of MAPK14-WT and MAPK14-MUT after co-transfection of mimic control or miR-124 mimic detected by dual-luciferase reporter gene assay. *$p < 0.05$ vs. the mice injected with mimic control. Measurement data were expressed as mean ± standard deviation, and an unpaired *t*-test was adopted to analyze the data between two groups. The experiment was repeated three times independently.

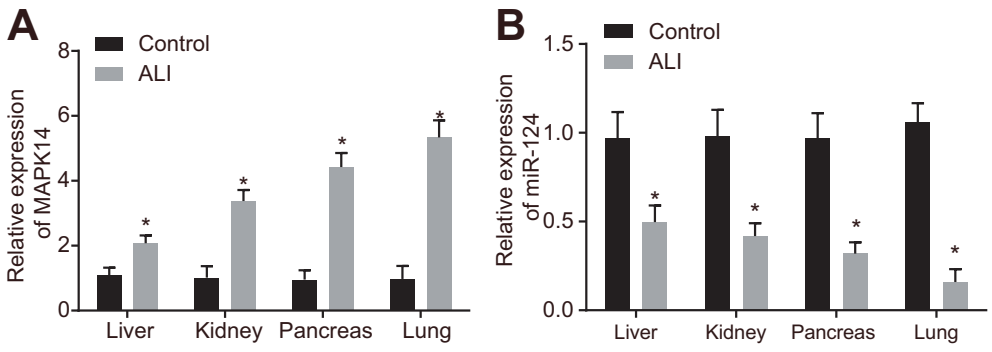

Fig. 3. MPAK14 expression increases and miR-124 expression decreases in lung tissues of ALI mice induced with LPS. A. differential expression of MAPK14 in liver, kidney, pancreas and lung tissues of normal mice and ALI mice induced with LPS, as determined by RT-qPCR. B. differential expression of miR-124 in liver, kidney, pancreas and lung tissues of normal mice and ALI mice induced with LPS, as determined by RT-qPCR. $*p < 0.05$ vs. the normal mice. Measurement data were expressed as mean ± standard deviation, and an unpaired *t*-test was adopted to analyze the data between two groups. n = 7. The experiment was repeated three times independently.

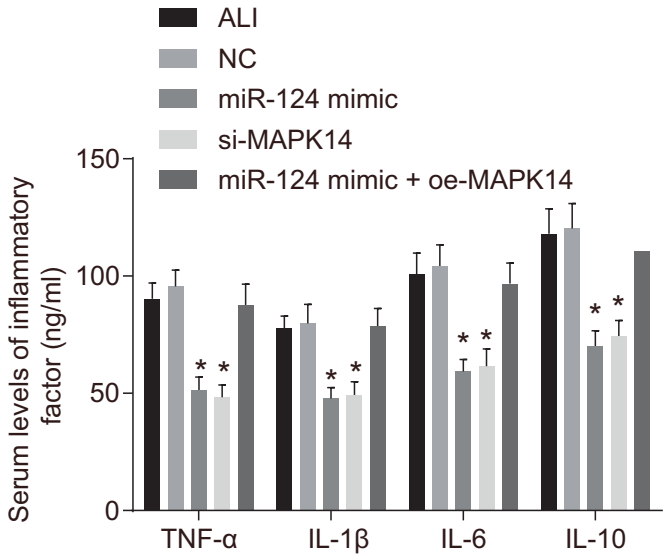

Fig. 4. Overexpression of miR-124 relieves inflammatory response in LPS-induced ALI mice by decreasing the expression of MAPK14. $*p < 0.05$ vs. mice ALI mice induced with LPS without any treatment. Measurement data were expressed as mean ± standard deviation. The comparison of data between multiple groups was analyzed by one-way ANOVA and subjected to Tukey's post hoc test. n = 7. The experiment was repeated three times independently.

tissues from ALI mice induced with LPS was detected by performing the Ki67 IHC assay (Fig. 7A), which suggested that the cell proliferation rate increased in response to miR-124 mimic or si-MAPK14 ($p < 0.05$), which could be blocked by co-treatment of oe-MAPKA14, suggesting that elevating miR-124 or depleting MAPK14 stimulated lung cell proliferation.

Besides, TUNEL staining was performed to detect lung cell apoptosis (Fig. 7B). The findings demonstrated that the lung cell apoptosis rate had significantly reduced following treatment of miR-124 mimic or treatment of si-MAPK14 in ALI mice ($p < 0.05$), which could be reversed after co-treatment of MAPKA14. Therefore, overexpression of miR-124 or silence of MAPK14 could inhibit lung cell apoptosis.

4. Discussion

ALI and acute respiratory distress syndrome (ARDS) account as the principal causes for high morbidity and mortality in severely ill patients of all age groups [18]. Various miRNAs are considered to function as a novel set of gene regulators, with significant roles in several intricate diseases including ALI. Many miRNAs have been viewed as new biomarkers and therapeutic targets for ALI/ARDS, which facilitates the comprehension of personalized medicine for patients with acute inflammatory lung diseases [19]. In our study, we identified that miR-124 could inhibit the MAPK signaling pathway by targeting MAPK14 in a mouse model of ALI, through which the symptoms of mice with ALI could be alleviated.

In our study, we findings demonstrated that the expression of MAPK14 increased evidently, while the expression of miR-124 decreased significantly in ALI mouse models. Evidence has indicated that the expression of miR-124 is prominently down-regulated in non-small cell lung cancer (NSCLC) [20]. Another study highlighted the importance of restoration of miR-124 in NSCLC in weakening migration, invasion and metastasis of cancer cells [21]. However, few studies have been conducted to investigate the relationship between miR-124 and ALI.

Moreover, our findings indicated that overexpression of miR-124 or silencing of MAPK14 could down-regulate the expression of inflammatory cytokines (TNF-α, IL-6, IL-1β, and IL-10) in ALI mice, thereby inhibiting or limiting the degree of tissue damage and pulmonary edema due to an inflammatory response. In consistency, another study has illustrated that the inflammatory cytokine is down-regulated upon over-expression of miR-124-3p through inhibition of nuclear factor-κB signaling [22]. p38 MAPK has already been identified to play important roles in inflammatory lung injury, which can regulate inflammatory cytokines, such as TNF-α, IL-1β, IL-6, and IL-10. However, the role of p38 MAPK in ALI remains unclear and requires further investigation [8].

Furthermore, our research demonstrated inhibition of that over-expressing miR-124 or silencing MAPK14 inhibited the expression along with the phosphorylation levels of ERK1/2, thereby inactivating the MAPK signaling pathway and the expression of pro-inflammatory response factor COX-2 in mice with ALI respectively. The potential reason exhibits that miR-124 inhibits the activation of MAPK signaling pathway by inhibiting the expression of MAPK14, thereby consequently reducing the expression of downstream pro-inflammatory response factors. A formal research has shown that up-regulation of ERK could be caused by miR-124 in squamous cell carcinoma [23]. A previous study has also found that miR-124 can regulate MAPK14/p38 in glioblastoma [24]. Meanwhile, the results of our study indicated that pulmonary cell proliferation could be promoted and pulmonary cell apoptosis could be inhibited by overexpression of miR-124 or silence of MAPK14. A previous report has specified p38 MAPK to be of vital significance for various cellular processes such as cell apoptosis, cell cycle arrest, cell growth inhibition and differentiation [25]. Besides, research another study has highlighted the ability of up-regulating miR-124 to extensively modulate cell apoptosis and the process of autophagy in Parkinson's disease, thereby reducing the loss of midbrain dopaminergic neurons [26].

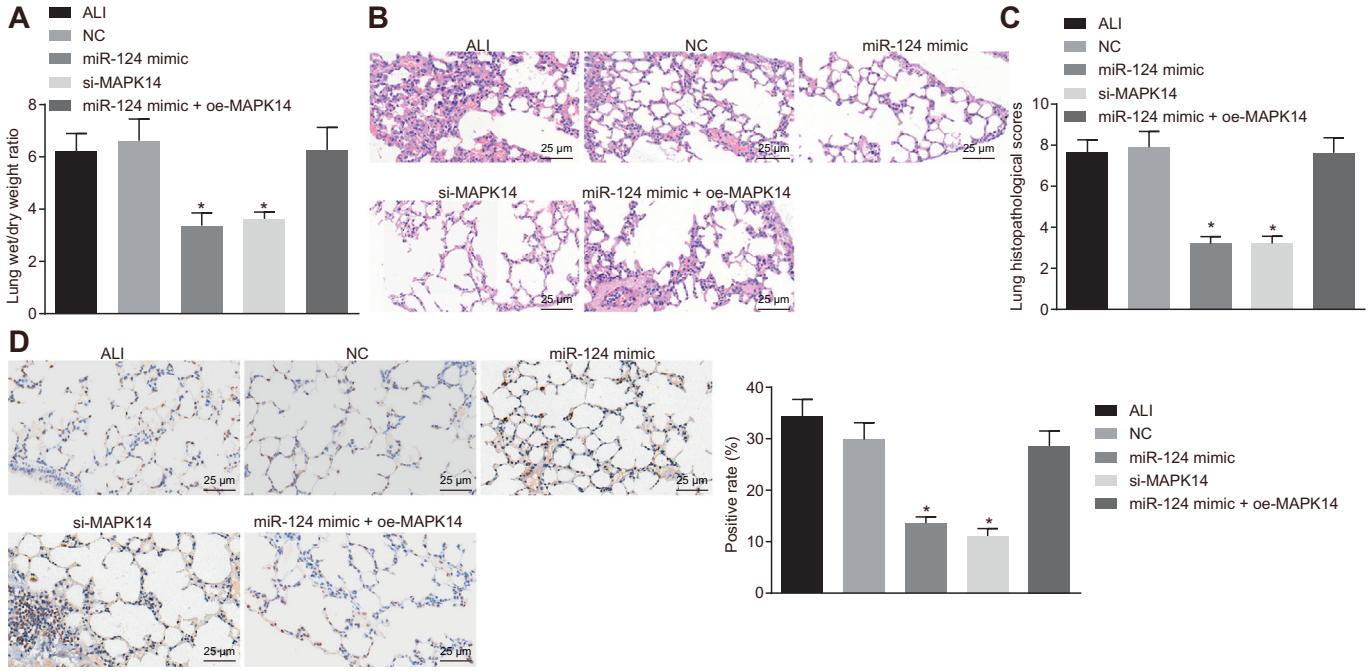

Fig. 5. Lung injury in ALI mice induced with LPS is relieved by overexpression of miR-124 or depletion of MAPK14. A. W/D ratio of lung tissues of ALI mice induced with LPS treated with blank plasmid, miR-124 mimic, si-MAPK14, or oe-MAPK14 (n = 3). B–C. HE staining of lung tissues from ALI mice induced with LPS treated with blank plasmid, miR-124 mimic, or si-MAPK14 (400×) (n = 7). D. expression of MAPK14 in ALI mice induced with LPS treated with the blank plasmid, miR-124 mimic, or si-MAPK14 (400×) (n = 7). *$p < 0.05$ vs. mice in ALI mice induced with LPS without treatment. Measurement data were expressed as mean ± standard deviation. The comparison of data between multiple groups was analyzed by one-way ANOVA and subjected to Tukey's post hoc test. The experiment was repeated three times independently.

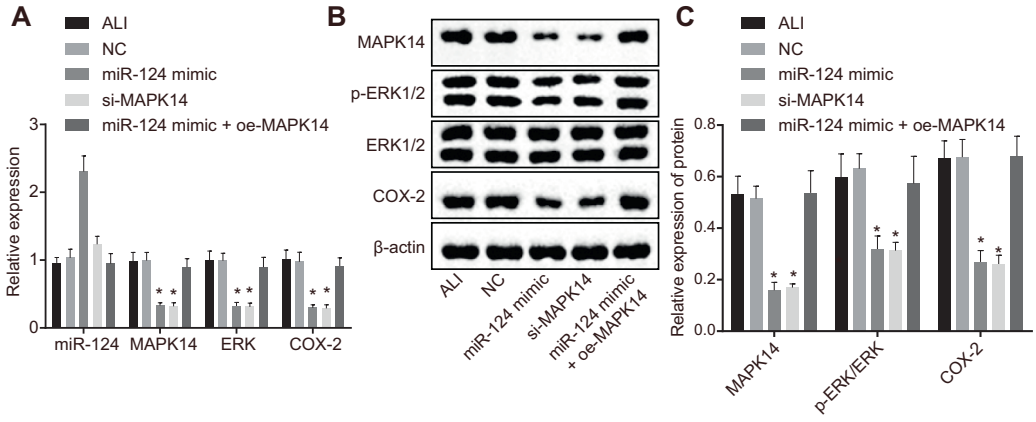

Fig. 6. miR-124 inhibits the activation of MAPK signaling pathway. A. expression of miR-124, MAPK14, ERK1/2, and COX-2 in lung tissue RNA of ALI mice induced with LPS treated with blank plasmid, miR-124 mimic, si-MAPK14, or oe-MAPK14, as determined by RT-qPCR. *$p < 0.05$ vs. ALI mice induced with LPS without treatment. B–C. expression of MAPK14, ERK1/2, and COX-2 as well as the phosphorylation extents of ERK1/2 in lung tissue RNA of ALI mice induced with LPS treated with blank plasmid, miR-124 mimic, si-MAPK14, or oe-MAPK14, as measured by Western blot analysis. *$p < 0.05$ vs. ALI mice induced with LPS without treatment. Measurement data were expressed as mean ± standard deviation. An unpaired *t*-test was adopted for data comparison between two groups. The comparison of data between multiple groups was analyzed by one-way ANOVA and subjected to Tukey's post hoc test. n = 7. The experiment was repeated three times independently.

5. Conclusion

To conclude, our research indicated that miR-124 inhibited the activation of MAPK pathway by inhibiting the expression of MAPK14, so as to reduce the severity of ALI mice in septic shock (Fig. 8). Our gathered evidence highlighted the potential of targeted regulation of miR-124 and MAPK14 as a novel strategy for ALI treatment. However, due to the limited condition, in vitro experiments were not performed, which propose the plan for a future study focused on exploring the underlying mechanism and ascertaining the results documented in this report.

Funding

None.

Acknowledgments

The authors thank the reviewers for their helpful comments.

Declaration of competing interest

The authors declare that they have no conflicts of interest.

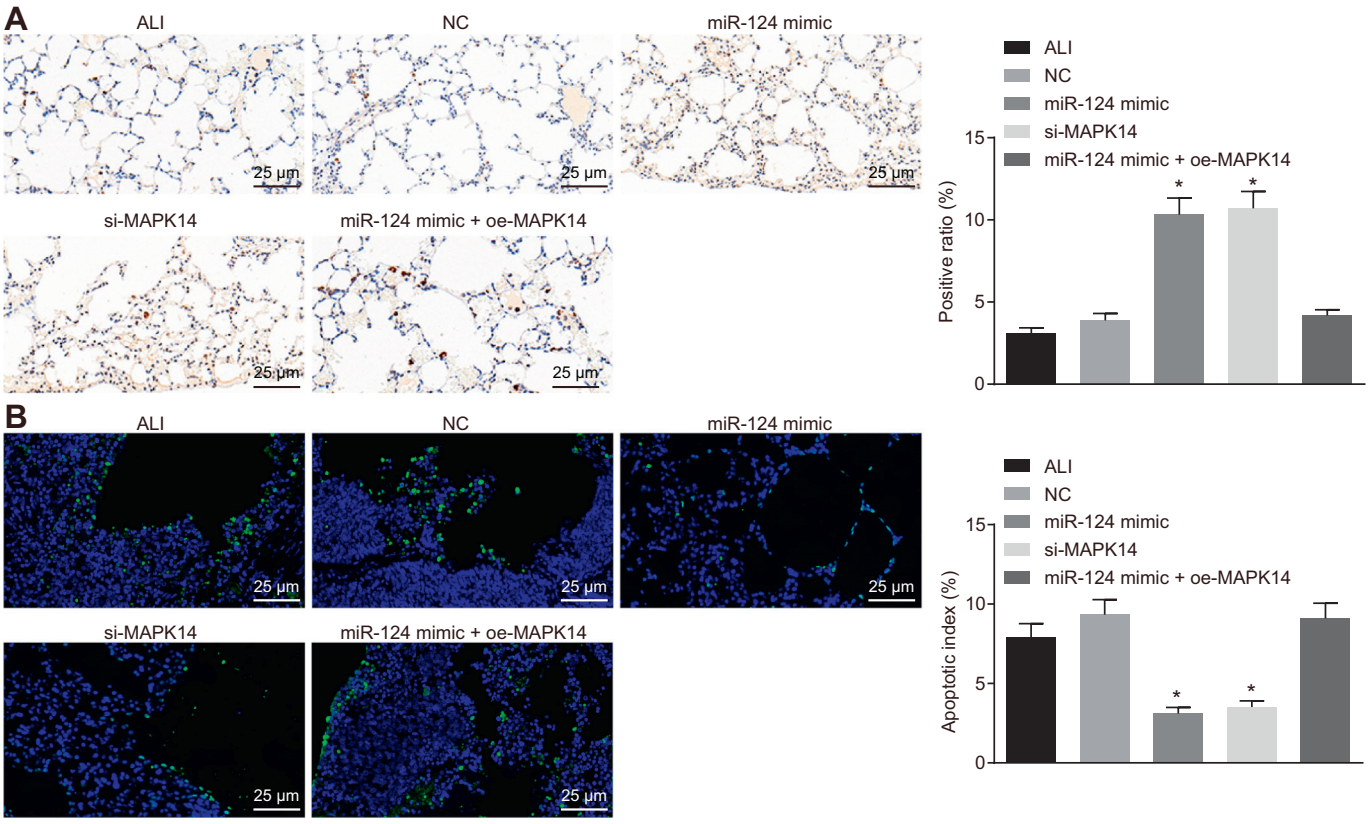

Fig. 7. Lung cell proliferation is promoted and lung cell apoptosis is inhibited by overexpressing miR-124 or silencing MAPK14 in ALI mice induced with LPS. A. lung cell proliferation in ALI mice induced with LPS treated with blank plasmid, miR-124 mimic, si-MAPK14, or oe-MAPK14 detected by Ki67 IHC (400×). B. lung cell apoptosis in ALI mice induced with LPS treated with blank plasmid, miR-124 mimic, si-MAPK14, or oe-MAPK14 detected by TUNEL staining (400×). *$p < 0.05$ vs. ALI mice induced with LPS without treatment. Measurement data were expressed as mean ± standard deviation. An unpaired *t*-test was adopted for comparing data between two groups. The comparison of data between multiple groups was analyzed by one-way ANOVA and subjected to Tukey's post hoc test. n = 7. The experiment was repeated three times independently.

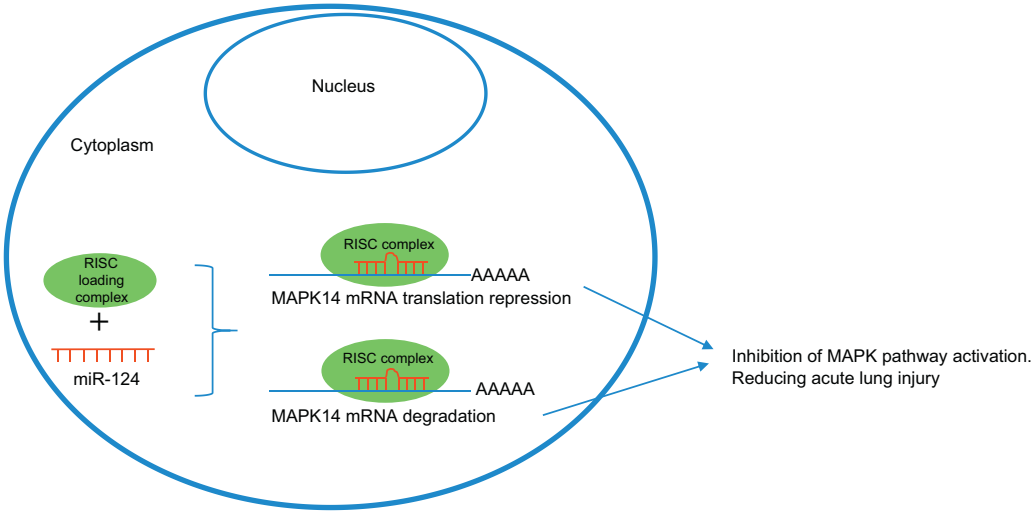

Fig. 8. The mechanism investigation demonstrated that miR-124 inhibited the expression of MAPK14, so as to reduce the severity of ALI mice in septic shock.

References

[1] Y. Yamanaka, K. Uchida, M. Akashi, Y. Watanabe, A. Yaguchi, S. Shimamoto, S. Shimoda, H. Yamada, M. Yamashita, H. Kimura, Mathematical modeling of septic shock based on clinical data, Theor Biol Med Model 16 (1) (2019) 5.

[2] M. Lipinska-Gediga, Sepsis and septic shock-is a microcirculation a main player? Anaesthesiol. Intensive Ther. 48 (4) (2016) 261–265.

[3] S. Fujishima, S. Gando, S. Daizoh, S. Kushimoto, H. Ogura, T. Mayumi, K. Takuma, J. Kotani, N. Yamashita, R. Tsuruta, N. Takeyama, S. Shiraishi, T. Araki, K. Suzuki, H. Ikeda, Y. Miki, Y. Suzuki, Y. Yamaguchi, N. Aikawa, G. Japanese Association for Acute Medicine Sepsis Registry Study, Infection site is predictive of outcome in acute lung injury associated with severe sepsis and septic shock, Respirology 21 (5) (2016) 898–904.

[4] Y. Butt, A. Kurdowska, T.C. Allen, Acute lung injury: a clinical and molecular review, Arch. Pathol. Lab. Med. 140 (4) (2016) 345–350.

[5] B.M. Elicker, K.T. Jones, D.M. Naeger, J.A. Frank, Imaging of acute lung injury, Radiol. Clin. N. Am. 54 (6) (2016) 1119–1132.

[6] J. Zhan, Y. Liu, Z. Zhang, C. Chen, K. Chen, Y. Wang, Effect of penehyclidine hydrochloride on expressions of MAPK in mice with CLP-induced acute lung injury,

Mol. Biol. Rep. 38 (3) (2011) 1909–1914.
[7] Y.H. Pei, X.M. Cai, J. Chen, B.D. Sun, Z.R. Sun, X. Wang, X.M. Qian, The role of p38 MAPK in acute paraquat-induced lung injury in rats, Inhal. Toxicol. 26 (14) (2014) 880–884.
[8] L.L. Xiong, Y. Tan, H.Y. Ma, P. Dai, Y.X. Qin, R.A. Yang, Y.Y. Xu, Z. Deng, W. Zhao, Q.J. Xia, T.H. Wang, Y.H. Zhang, Administration of SB239063, a potent p38 MAPK inhibitor, alleviates acute lung injury induced by intestinal ischemia reperfusion in rats associated with AQP4 downregulation, Int. Immunopharmacol. 38 (2016) 54–60.
[9] N. Umasuthan, S.D. Bathige, J.K. Noh, J. Lee, Gene structure, molecular characterization and transcriptional expression of two p38 isoforms (MAPK11 and MAPK14) from rock bream (Oplegnathus fasciatus), Fish Shellfish Immunol. 47 (1) (2015) 331–343.
[10] L. Smirnova, A. Grafe, A. Seiler, S. Schumacher, R. Nitsch, F.G. Wulczyn, Regulation of miRNA expression during neural cell specification, Eur. J. Neurosci. 21 (6) (2005) 1469–1477.
[11] S. Rajasekaran, D. Pattarayan, P. Rajaguru, P.S. Sudhakar Gandhi, R.K. Thimmulappa, MicroRNA regulation of acute lung injury and acute respiratory distress syndrome, J. Cell. Physiol. 231 (10) (2016) 2097–2106.
[12] M. Du, W. Chen, W. Zhang, X.K. Tian, T. Wang, J. Wu, J. Gu, N. Zhang, Z.W. Lu, L.X. Qian, Q. Fei, Y. Wang, F. Peng, X. He, L. Yin, TGF-? regulates the ERK/MAPK pathway independent of the SMAD pathway by repressing miRNA-124 to increase MALAT1 expression in nasopharyngeal carcinoma, Biomed. Pharmacother. 99 (2018) 688–696.
[13] X. Wang, Y. Liu, X. Liu, J. Yang, G. Teng, L. Zhang, C. Zhou, MiR-124 inhibits cell proliferation, migration and invasion by directly targeting SOX9 in lung adenocarcinoma, Oncol. Rep. 35 (5) (2016) 3115–3121.
[14] D. Szklarczyk, A. Franceschini, S. Wyder, K. Forslund, D. Heller, J. Huerta-Cepas, M. Simonovic, A. Roth, A. Santos, K.P. Tsafou, M. Kuhn, P. Bork, L.J. Jensen, C. von Mering, STRING v10: protein-protein interaction networks, integrated over the tree of life, Nucleic Acids Res. 43 (Database issue) (2015) D447–D452.
[15] P. Shannon, A. Markiel, O. Ozier, N.S. Baliga, J.T. Wang, D. Ramage, N. Amin, B. Schwikowski, T. Ideker, Cytoscape: a software environment for integrated models of biomolecular interaction networks, Genome Res. 13 (11) (2003) 2498–2504.
[16] L.Y. Jin, C.F. Li, G.F. Zhu, C.T. Wu, J. Wang, S.F. Yan, Effect of siRNA against NF-kappaB on sepsis-induced acute lung injury in a mouse model, Mol. Med. Rep. 10 (2) (2014) 631–637.
[17] C. Qiao, Q. Zhang, Q. Jiang, T. Zhang, M. Chen, Y. Fan, J. Ding, M. Lu, G. Hu, Inhibition of the hepatic Nlrp3 protects dopaminergic neurons via attenuating systemic inflammation in a MPTP/p mouse model of Parkinson's disease, J. Neuroinflammation 15 (1) (2018) 193.
[18] L. Ionescu, R.N. Byrne, T. van Haaften, A. Vadivel, R.S. Alphonse, G.J. Rey-Parra, G. Weissmann, A. Hall, F. Eaton, B. Thebaud, Stem cell conditioned medium improves acute lung injury in mice: in vivo evidence for stem cell paracrine action, Am. J. Physiol. Lung Cell. Mol. Physiol. 303 (11) (2012) L967–L977.
[19] T. Zhou, J.G. Garcia, W. Zhang, Integrating microRNAs into a system biology approach to acute lung injury, Transl. Res. 157 (4) (2011) 180–190.
[20] Z. Li, X. Wang, W. Li, L. Wu, L. Chang, H. Chen, miRNA-124 modulates lung carcinoma cell migration and invasion, Int. J. Clin. Pharmacol. Ther. 54 (8) (2016) 603–612.
[21] L. Zu, Y. Xue, J. Wang, Y. Fu, X. Wang, G. Xiao, M. Hao, X. Sun, Y. Wang, G. Fu, J. Wang, The feedback loop between miR-124 and TGF-beta pathway plays a significant role in non-small cell lung cancer metastasis, Carcinogenesis 37 (3) (2016) 333–343.
[22] Z. Zhao, Y. Han, Z. Zhang, W. Li, X. Ji, X. Liu, J. Jin, S. Xu, H. Cui, Z. Cheng, Q. Wang, X. Wang, X. Guo, Y. Wang, H. Liu, Total glucosides of paeony improves the immunomodulatory capacity of MSCs partially via the miR-124/STAT3 pathway in oral lichen planus, Biomed. Pharmacother. 105 (2018) 151–158.
[23] K. Yamane, M. Jinnin, T. Etoh, Y. Kobayashi, N. Shimozono, S. Fukushima, S. Masuguchi, K. Maruo, Y. Inoue, T. Ishihara, J. Aoi, Y. Oike, H. Ihn, Down-regulation of miR-124/-214 in cutaneous squamous cell carcinoma mediates abnormal cell proliferation via the induction of ERK, J. Mol. Med. (Berl) 91 (1) (2013) 69–81.
[24] V. Mucaj, S.S. Lee, N. Skuli, D.N. Giannoukos, B. Qiu, T.S. Eisinger-Mathason, M.S. Nakazawa, J.E. Shay, P.P. Gopal, S. Venneti, P. Lal, A.J. Minn, M.C. Simon, L.K. Mathew, MicroRNA-124 expression counteracts pro-survival stress responses in glioblastoma, Oncogene 34 (17) (2015) 2204–2214.
[25] X. Sui, N. Kong, L. Ye, W. Han, J. Zhou, Q. Zhang, C. He, H. Pan, p38 and JNK MAPK pathways control the balance of apoptosis and autophagy in response to chemotherapeutic agents, Cancer Lett. 344 (2) (2014) 174–179.
[26] H. Wang, Y. Ye, Z. Zhu, L. Mo, C. Lin, Q. Wang, H. Wang, X. Gong, X. He, G. Lu, F. Lu, S. Zhang, MiR-124 regulates apoptosis and autophagy process in MPTP model of Parkinson's disease by targeting to Bim, Brain Pathol. 26 (2) (2016) 167–176.